DOI: 10.1002/adma.200602461

Highly Ordered Nanoporous Thin Films from Cleavable Polystyrene-*block*-poly(ethylene oxide)**

By *Mingfu Zhang*, *Ling Yang*, *Serkan Yurt*, *Matthew J. Misner*, *Jiun-Tai Chen*, *E. Bryan Coughlin*, *Dhandapani Venkataraman*,* and *Thomas P. Russell**

Nanoporous polymer thin films produced from ordered block copolymer precursors have received considerable attention, because they can be used in many applications including templating, separation, catalysis, and sensors.[1] Since 1988,[2] various block copolymers have been used to prepare nanoporous thin films via the selective removal of degradable minor components from self-assembled block copolymers. For cylinder-forming block copolymers, selective etching of the cylindrical microdomain in an ordered block copolymer results in the formation of nanoscopic channels. Specially, if the etchable cylinders are orientated normal to the film surface, removal of the cylinders will lead to the nanolithographic masks used in block-copolymer lithography.[3]

Currently, the generation of nanoporous materials from ordered block copolymers relies on a selective etching protocol that does not compromise the integrity of the matrix material. Ozonolysis,[2,4] UV degradation,[5,6] reactive ion etching (RIE),[7] and chemical etching[8] are the methods that are commonly used for the removal of minor components to create nanopores. However, the number of polymers that can be degraded under mild reaction conditions in the thin-film state is limited. The preparation of nanoporous thin films from block copolymers without a degradable component requires a rational design of the polymer. In principle, to generate nanopores from self-assembled block copolymers, it is not necessary to degrade the backbone bonds in the minor component; rather, a cleavage of the juncture between two immiscible blocks is sufficient.[9–12] Therefore, if one could put a cleavable juncture into a block copolymer; the cleavage will not depend on the chemical nature of the minor component and should be applicable to a much larger variety of block copolymers. Cleavage of the juncture point of block copolymer in the ordered state followed by removal of the minor component via selective solvents is therefore a very promising strategy for the generation of nanoporous structures.

For most of the nanoporous polymer thin films prepared to date, one of the major problems is the lack of long-range order in the nanopore array, which prevents them from being used in applications where addressability is required (e.g., magnetic storage devices). Long-range order in thin films of the precursor block copolymers is a prerequisite for obtaining nanoporous materials with well-ordered pores. We have recently demonstrated that the solvent-annealing of thin films of polystyrene-*block*-poly(ethylene oxide) (PS-*b*-PEO) diblock copolymers leads to highly ordered arrays of PEO cylinders oriented normal to the film surface.[13] The long-range lateral order and the orientation in the annealed PS-*b*-PEO thin films arise from the strong nonfavorable interactions between PS and PEO, enhanced mobility caused by the presence of solvent, as well as the directionality of solvent evaporation. The subsequent removal of the PEO domain will lead to nanoporous films with identical long-range order. However, the poor degradability of PEO prevents the direct generation of nanopores from ordinary PS-*b*-PEO. Mao and Hillmyer recently reported the successful use of hydroiodic acid to degrade PEO in the bulk sample of PS-*b*-PEO,[14] but the harsh reaction conditions they used are not applicable to thin films.

To impart the degradability to the PS-*b*-PEO system, we recently synthesized a triblock copolymer, polystyrene-*b*-poly(methyl methacrylate)-*b*-poly(ethylene oxide) (PS-*b*-PMMA-*b*-PEO), where PS is the major component and PMMA and PEO are minor components.[15] By taking the advantage of the photodegradability of the PMMA mid-block, nanoporous thin films with excellent long-range order suitable for block copolymer lithography were prepared. In this method, the degradation efficiency depends critically on the molecular weight and phase behavior of the PMMA block, and only when PMMA formed a distinct microdomain did efficient degradation occur.

In this paper, we show that by placing a cleavable juncture, a triphenylmethyl (trityl) ether linkage, between PS and PEO,

[*] Prof. D. Venkataraman, S. Yurt
Department of Chemistry
University of Massachusetts
Amherst, MA 01003 (USA)
E-mail: dv@chem.umass.edu
Prof. T. P. Russell, Dr. M. Zhang, Dr. L. Yang, Dr. M. J. Misner, J.-T. Chen, Prof. E. B. Coughlin
Department of Polymer Science and Engineering
University of Massachusetts
Amherst, MA 01003 (USA)
E-mail: russell@mail.pse.umass.edu

[**] We thank Dr. Xuefa Li and Dr. Jin Wang (Argonne National Laboratory) for their assistance with the GISAXS measurements. We also acknowledge Dr. Cuihong Jiang (Department of Polymer Science and Engineering, University of Massachusetts Amherst) for the assistance in IR measurements. Yeon Sik Jung and Prof. Caroline Ross from MIT are acknowledged for providing the patterned substrates. This work was supported by NSF-supported MRSEC at the University of Massachusetts, Seagate Technologies (M.Z.), and the U.S. Department of Energy Basic Energy Science (J.-T.C., T.P.R.).

ADVANCED MATERIALS

highly ordered nanoporous thin films could be prepared directly from PS-*b*-PEO diblock copolymers. It is known that the trityl ether linkage can be readily cleaved by Brønsted or Lewis acids at ambient conditions.[16] This provides a general strategy for the site-specific scission of block copolymers, not limited to PS-*b*-PEO. Different from the triblock copolymer method, in which the length of the central PMMA block has to be controlled in order to form a distinct phase, the cleavable trityl ether does not change the overall phase-separation characteristics of block copolymers, because of the negligible volume fraction of the juncture.

The chemical structure of the cleavable PS-*b*-PEO with a trityl ether juncture is shown in Figure 1a. The polymer we used has the number-average molecular weight of

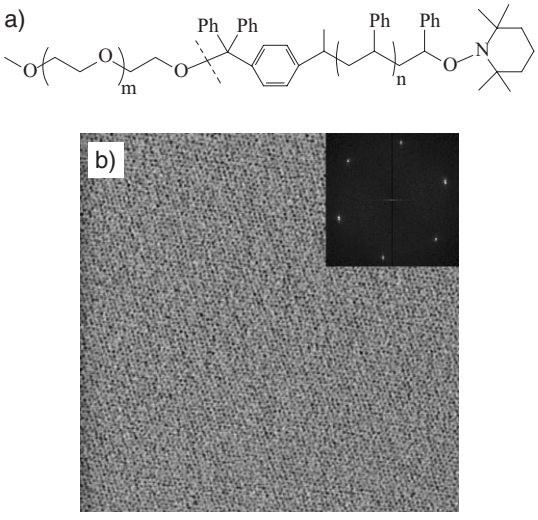

Figure 1. a) Chemical structure of cleavable PS-*b*-PEO (the dash line shows the point where scission occurs); b) Scanning force microscopy (SFM) phase image (2 μm × 2 μm) of PS-*b*-PEO thin film (ca. 25 nm) containing KI (O/K = 64) on silicon wafer after solvent-annealing for 48 h. The inset shows the corresponding Fourier transform.

19.6 kg mol^{-1} and 5.0 kg mol^{-1} for PS and PEO blocks respectively, with a polydispersity index of the copolymer of 1.18. The synthesis of this diblock copolymer, using nitroxide-mediated living radical polymerization, was described previously.[17] We have previously shown that this PS-*b*-PEO diblock copolymer can be rapidly cleaved into its constituent blocks in solution under mild reaction conditions.

In our previous publications,[13,18] it has been shown that solvent-annealing of thin films of cylinder-forming PS-*b*-PEO resulted in the normal orientation of PEO cylinders, as well as, long-range lateral order. We have found that humidity plays a critical role in the orientation and ordering process.[15] When solvent-annealing was carried out under controlled humidity atmosphere (70–90 % relative humidity (RH)), PEO cylinders were oriented normal to the film surface with long-range lateral order; while under low humidity conditions, parallel orientation was achieved.

Very recently, salt complexation within cylinder-forming PS-*b*-PEO thin films was found to affect the ordering process during solvent-annealing/evaporation, significantly enhancing the lateral order of PEO cylinders.[19] High humidity is not needed for the salt-complexed thin films, and the solvent-annealing can be carried out under dry conditions. The enhanced nonfavorable interactions between PS and PEO caused by the complexation of PEO with salt,[20,21] coupled with the high mobility of polymer chains in the presence of solvent, gives rise to the high degree of lateral ordering in the resultant film. In this work, a small amount of potassium iodide (KI, with the molar ratio of O/K = 64) was added, and the PS-*b*-PEO thin films were solvent-annealed using benzene under N_2.

A typical scanning force microscopy (SFM) image of the salted PS-*b*-PEO thin film after solvent-annealing under N_2 is shown in Figure 1b. Different from the unsalted PS-*b*-PEO thin films annealed under high RH (70–90 %), which shows clear phase contrast in the SFM phase image because of the depression of PEO microdomains,[13,15,18] thin films of salted PS-*b*-PEO show poorer phase contrast, most probably because of the decreased depression of PEO cylinders in the absence of water during solvent evaporation. Fourier transformation of the SFM image (see the inset of Fig. 1b) still shows a six-spot pattern, indicating the high degree of translational and orientational order over the 2 μm × 2 μm area. The *d*-spacing was determined to be ca. 21 nm based on the Fourier transform.

To generate nanopores from the annealed PS-*b*-PEO thin films, cleavage of the trityl ether juncture followed by the selective removal of PEO from the films were performed. Two key requirements must be met in order to generate nanoporous thin films with the translational and orientational orders identical to those of the precursor film: i) the cleavable juncture must be physically accessible to the etching reagent, which is trifluoroacetic acid (TFA) in this study; and ii) the matrix material must be able to support the resultant nanoporous structure. For the annealed PS-*b*-PEO thins films, the orientation of the PEO cylinders normal to the film surface facilitates the diffusion of hydrophilic etching regent (e.g., TFA, which is a solvent for PEO but a nonsolvent for PS) to the PS/PEO interface through the cylindrical PEO domains, ensuring high cleavage efficiency. The strong nonfavorable interaction between PS and PEO, which is further enhanced by salt complexation, ensures a sharp PS/PEO interface that is crucial for the site-specific scission. The normal orientation of the cylindrical PEO microdomains also offers a physical pathway for the removal of PEO homopolymer after cleavage. In addition, the glassy PS matrix can support the resultant nanoporous structure.

Our experiments shows that exposure of unsalted PS-*b*-PEO thin films to TFA vapor readily induced the cleavage of the trityl ether junction. Because of the mobility imparted by the TFA vapor, detached PEO homopolymer chains migrated to the film surface forming crystals, as clearly shown in both the optical microscopy images (Fig. 2a) and SFM images

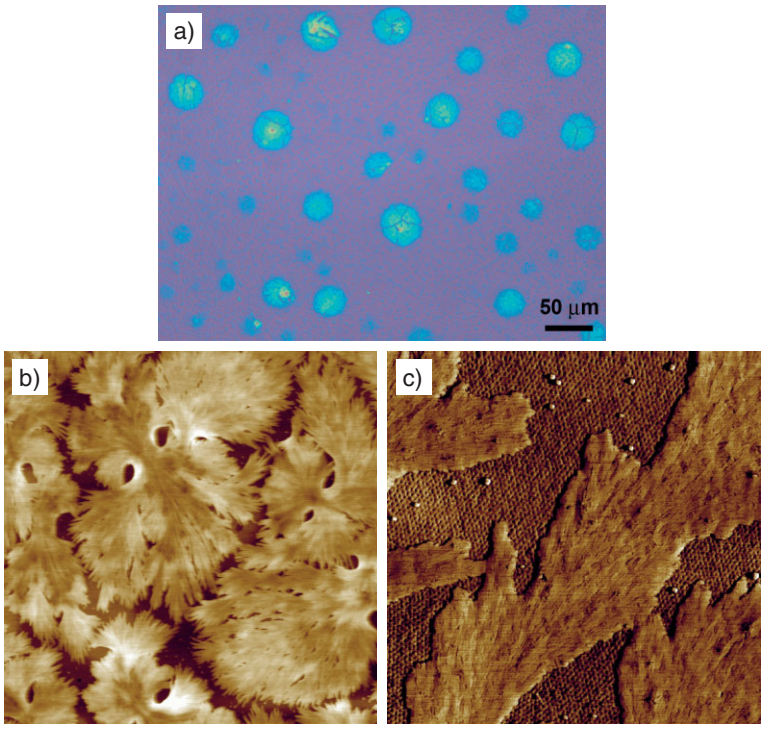

Figure 2. a) Microscopy image of PS-*b*-PEO thin film (ca. 25 nm) on silicon wafer after exposure to TFA vapor for 4 h; b) SFM height image (10 μm × 10 μm), and c) phase image (2 μm × 2 μm) of the PEO crystals formed at the surface of the film after TFA vapor treatment.

(Fig. 2b and c). However, exposure of the salted PS-*b*-PEO thin films to TFA vapor did not produce efficient cleavage, as compared to the unsalted samples. Most likely, the pseudo-crown ether complex between PEO and salts[22] retarded the cleavage of trityl ether linkage and/or the migration of PEO chains. The potassium ions effectively "crosslink" the PEO chains via complexation, limiting the physical access of TFA to the juncture. Thus, the salted PS-*b*-PEO thin films were immersed in a mixture of methanol and water (v/v = 10:1) before the exposure to TFA vapor, with the intent to break the complexation between the potassium ion and ethylene oxide by water and to swell the PEO chains in the selective solvent mixture. As expected, after the treatment with the mixture of methanol and water, exposure of the thin films to TFA vapor readily cleaved the trityl ether juncture and the detached PEO chains migrated to the surface of the film (as indicated by the formation of PEO crystals). In addition, because TFA is a nonsolvent for PS, the matrix remained intact and, thus, the translational and orientational orders were not affected by the TFA vapor treatment. As clearly shown in Figure 2c, the nanoporous film shows the same ordering as the precursor PS-*b*-PEO thin film.

The PEO crystals, formed on the surface of the polymer film after the cleavage of the trityl ether juncture, can be easily removed by washing with methanol or a mixture of methanol and water (v/v = 10:1). Optical microscopy and SFM measurements showed that a clean surface was obtained after washing. The SFM phase image (Fig. 3a) shows that the nanoporous thin film has exactly the same lateral order and *d* spacing as those of the precursor PS-*b*-PEO thin film. The removal of the PEO enhanced the phase contrast significantly, as shown in Figure 3a. After washing, the nanoporous thin films were exposed to TFA vapor again, aiming to cleave unreacted trityl ether junctions. However, no PEO crystals were observed after the second TFA vapor treatment, indicating the high efficiency of cleavage during the first exposure to TFA vapor.

Using a buffered HF solution, the nanoporous thin films were detached from the silicon substrate having a thick (200 nm) silicon oxide layer and transferred to copper grids for transmission electron microscopy (TEM) measurements. The TEM image (Fig. 3b) clearly shows the nanoporous structure. Based on the TEM image, the average pore size was determined to be ca. 12 nm in diameter, with a very narrow pore size distribution.

The successful removal of PEO from ordered PS-*b*-PEO thin films via TFA vapor treatment followed by washing is further demonstrated by IR spectroscopy measurements. In the original PS-*b*-PEO thin film, absorptions of the C–O–C stretching and CH_2 rocking modes in PEO were clearly observed at the wavelength of 1117 and 965 cm^{-1}, respectively. After removal of PEO, both peaks disappeared, as shown in Figure 4.

Pore generation was further confirmed by static grazing incidence small-angle X-ray scattering (GISAXS) on thin films before and after removal of the PEO. Figure 5a and b show two GISAXS patterns, where the angle of incidence was above the critical angle of the polymer film and, thus, the X-ray beam fully penetrated through the film. The sharp Bragg rods (vertical streaks) in the GISAXS patterns corre-

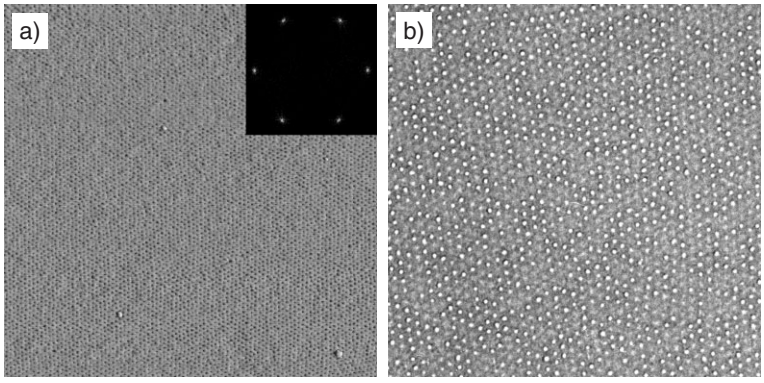

Figure 3. a) SFM phase image (2 μm × 2 μm) and b) TEM image (1 μm × 1 μm) of nanoporous PS thin film (ca. 25 nm).

ADVANCED MATERIALS

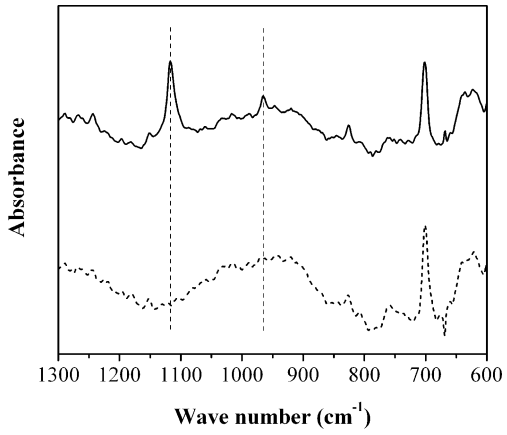

Figure 4. External reflection IR spectra of PS-*b*-PEO thin film with the thickness of 80 nm (solid line) and the corresponding nanoporous PS thin film (dash line).

spond to the reflections from a 2D lattice of cylinders of finite length oriented normal to the film surface. Before the removal of PEO, only first- and second-order reflections were observed; whereas after pore generation, higher-order reflections were clearly observed. The reflections from the nanoporous thin film are located at the scattering vectors of $1{:}\sqrt{3} : \sqrt{4} : \sqrt{7}$ relative to the first-order reflection, characteristic of hexagonally close-packed cylindrical microdomains. For a thicker nanoporous film (thickness of ca. 60 nm), GISAXS measurement (data not shown) showed up to the sixth-order reflection. The existence of many higher-order reflections, together with the sharpness of the Bragg rods, indicates the exceptionally high degree of lateral order in the resultant nanoporous thin films.

The intensity profiles parallel to the surface of the film (q_y direction) of the GISAXS patterns shown in Figure 5a and b are plotted in Figure 5c and d, respectively. The intensity of the primary scattering peak for the nanoporous sample is about one order of magnitude higher than the precursor PS-*b*-PEO thin film, consistent with the significant increase in the electron density difference caused by the formation of the nanopores. From the scattering vector of the primary reflection, the *d* spacing was calculated to be ca. 22 nm, and no change in the *d* spacing was observed during pore generation, which is consistent with the SFM observations.

Occasionally cracks were found in the nanoporous thin films, more than likely because the matrix consists of low-molecular-weight PS. Improvements to the mechanical stability of these nanoporous thin films may be achieved via crosslinking of the PS matrix or by adding PS homopolymer of high molecular weight into block copolymers.

By using the two-step process described above, we could easily monitor the cleavage of the trityl ether juncture and removal of PEO by using various microcopy techniques. It has been shown that the trityl ether linkage can be readily cleaved in solution by using various acids, such as formic acid,[23] acetic acid,[24] TFA,[25] and hydrochloric acid.[26] In principle, we can combine the cleavage and washing into one step, simply by immersing the thin film in a selective washing solvent (which should be a good solvent for PEO but a nonsolvent for PS) containing a suitable cleaving agent. In the simplest case, one may use an acid, such as TFA or acetic acid, as both the cleaving agent and the washing solvent.

Immersion of annealed PS-*b*-PEO thin films in TFA resulted in nanoporous thin films directly, because PEO homopolymer was dissolved in TFA after it was detached from the PS matrix. As a more commonly used organic acid, acetic acid was also used. However, when the thin films of cleavable PS-*b*-PEO were immersed in acetic acid, the surface topography was changed and the ordering was destroyed. Alternatively one can immerse PS-*b*-PEO thin films in methanol-containing cleaving reagents, such as hydrochloric acid. When a mixture of methanol and hydrochloric acid (37.4 %, volume ratio of methanol and HCl solution is 10:1) was used, the trityl ether linkage was also cleaved and nanoporous PS thin films were obtained. Thus by choosing the proper acid or the mixture of solvent with a suitable acid, we can generate nanoporous thin films in a single step.

It has been shown that substrates with topographic features, such as well-defined troughs, can bias the orientation of the lattices of block copolymers, opening the possibility of sectoring surfaces into areas of highly ordered microdomains.[13,27–33] By combining the solvent-induced orientation and ordering of the microdomains in thin films of cleavable PS-*b*-PEO diblock copolymers with the confinement imparted by a series of parallel troughs (with square-wave profile) etched in silicon, we were able to produce highly ordered arrays of hexagonally packed PEO cylindrical microdomains, where the arrays in adjoining troughs were in orientational registry. After removal of PEO by using the two-step process described above, nearly defect-free arrays of nanopores were obtained within the troughs, as shown in Figure 6a and b. Fourier transforms of the SFM images are shown as the insets, where six-point patterns with multiple higher-order reflections are obtained, characteristic of the exceptional long-range order. Clearly, the lattice of nanopores is highly aligned with respect to the trough walls. Similar results were obtained when patterned substrates with circumferential troughs were used. Thus, by topographically sectoring a surface with standard lithographic processes, addressable nanopore arrays can be readily produced with a high degree of lateral order and a well-defined lattice orientation. Such hierarchical structures may find applications in fields such as patterned magnetic recording media.

In conclusion, we have shown in this paper that, by introducing a cleavable trityl ether juncture between PS and PEO, highly ordered nanoporous thin films can be easily prepared from cylinder-forming PS-*b*-PEO diblock copolymers. The removal of PEO from solvent-annealed PS-*b*-PEO thin films can be carried out in a simple two or one-step process. Patterned substrates can also be used. This allows templates for block-copolymer lithography and opens routes to the fabrication of addressable media.

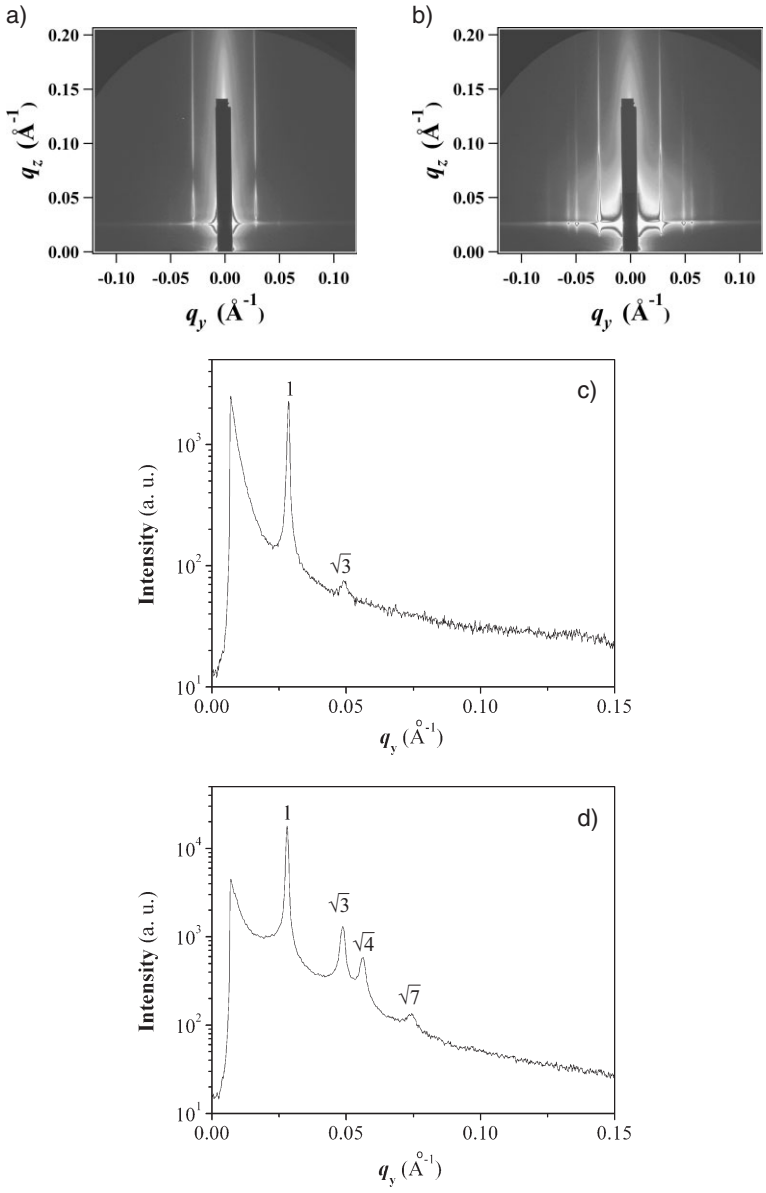

Figure 5. GISAXS patterns of a) thin film (ca. 25 nm) of cleavable PS-*b*-PEO containing KI (O/K = 64) and b) the corresponding nanoporous PS thin film; c,d) Intensity scans along q_y of the GISAXS patterns shown in (a) and (b), respectively.

Experimental

PS-*b*-PEO possessing a trityl ether juncture, with a molecular weight of 24.6 kg mol^{-1} (19.6 kg mol^{-1} for the PS block and 5.0 kg mol^{-1} for the PEO block) and a polydispersity index of 1.18 was used in this study. Potassium iodide was added to the copolymer by mixing equal volumes of the copolymer solution in tetrahydrofuran and the salt solution in methanol. After 12 h the salt-complexed copolymer was precipitated by the addition of hexane. The precipitate was separated via centrifugation, dried, and redissolved in benzene. Solutions of the block copolymer with and without added salt were spin-coated onto cleaned silicon substrates where the film thickness was controlled by the spinning rate and/or the solution concentration.

The salted PS-*b*-PEO thin films were solvent-annealed for 48 h in a benzene-saturated chamber that was placed in a glove-box filled with dry N_2. For unsalted PS-*b*-PEO thin films, solvent-annealing was carried out under high RH (70–90 %). After solvent-annealing, the salted thin films were immersed in the mixture of methanol and water (v/v = 10:1) for 8 h. Then the films were exposed to TFA vapor in a chamber for 4 h, followed by washing with methanol for another 4 h. Alternatively, removal of PEO was achieved by immersing the annealed PS-*b*-PEO thin films in TFA for 4–6 h.

SFM images were obtained using a Digital Instruments Dimension 3000 scanning force microscope operating in the tapping mode. TEM studies were performed on a JEOL 100CX electron microscope operated at 100 kV. For the TEM measurements, the samples were prepared on silicon substrates with a thick layer of silicon oxide. The polymer film was then floated onto the surface of an aqueous solution containing 5 wt % HF, transferred to a water bath, and then retrieved with a Cu grid for TEM measurement. GISAXS measurements were performed at the 8-ID-E beamline at the Advanced Photon Source (Argonne National Laboratory) with an X-ray wavelength of 1.664 Å. External reflection IR spectroscopy measurements were carried out on a Perkin Elmer Fourier transform IR (FTIR) spectrometer (SPECTRUM 2000). 256 scans were taken to obtain the spectra with a resolution of 4 cm^{-1}. For IR measurements, PS-*b*-PEO thin films of ca. 80 nm in thickness were prepared on gold-coated silicon wafers (35 nm gold on a 2 nm layer of chromium).

Received: October 30, 2006
Revised: December 21, 2006
Published online: May 15, 2007

[1] M. A. Hillmyer, *Adv. Polym. Sci.* **2005**, *190*, 137.
[2] J. S. Lee, A. Hirao, S. Nakahama, *Macromolecules* **1988**, *21*, 274.
[3] C. J. Hawker, T. P. Russell, *MRS Bull.* **2005**, *30*, 952.
[4] P. Mansky, C. K. Harrison, P. M. Chaikin, R. A. Register, N. Yao, *Appl. Phys. Lett.* **1996**, *68*, 2586.
[5] T. Thurn-Albrecht, R. Steiner, J. DeRouchey, C. M. Stafford, E. Huang, M. Bal, M. Tuominen, C. J. Hawker, T. P. Russell, *Adv. Mater.* **2000**, *12*, 787.
[6] T. Thurn-Albrecht, J. Schotter, G. A. Kastle, N. Emley, T. Shibauchi, L. Krusin-Elbaum, K. Guarini, C. T. Black, M. T. Tuominen, T. P. Russell, *Science* **2000**, *290*, 2126.
[7] R. Olayo-Valles, M. S. Lund, C. Leighton, M. A. Hillmyer, *J. Mater. Chem.* **2004**, *14*, 2729.
[8] J. M. Leiston-Belanger, T. P. Russell, E. Drockenmuller, C. J. Hawker, *Macromolecules* **2005**, *38*, 7676.
[9] J. T. Goldbach, T. P. Russell, J. Penelle, *Macromolecules* **2002**, *35*, 4271.
[10] J. T. Goldbach, K. A. Lavery, J. Penelle, T. P. Russell, *Macromolecules* **2004**, *37*, 9639.
[11] M. Lee, M.-H. Park, N.-K. Oh, W.-C. Zin, H.-T. Jung, D. K. Yoon, *Angew. Chem. Int. Ed.* **2004**, *43*, 6466.
[12] C.-A. Fustin, B. G. G. Lohmeijer, A.-S. Duwez, A. M. Jonas, U. S. Schubert, J.-F. Gohy, *Adv. Mater.* **2005**, *17*, 1162.
[13] S. H. Kim, M. J. Misner, T. Xu, M. Kimura, T. P. Russell, *Adv. Mater.* **2004**, *16*, 226.
[14] H. Mao, M. A. Hillmyer, *Macromolecules* **2005**, *38*, 4038.

ADVANCED MATERIALS

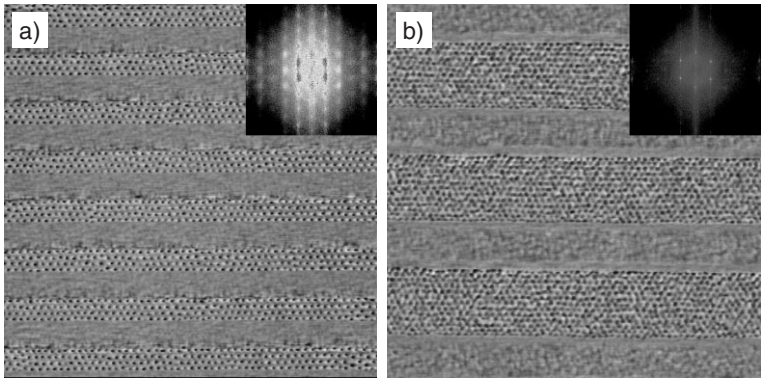

Figure 6. SFM phase images (1.5 mm × 1.5 mm) and the corresponding Fourier transform (insets) of nanoporous PS thin films on patterned substrates with troughs of different sizes: a) trough width of ca. 85 nm and depth of ca. 75 nm; b) trough width of ca. 270 nm and depth of ca. 75 nm. Note that the nanoporous film in (a) originated from an unsalted PS-PEO film, and the nanoporous film in (b) originated from a salted PS-*b*-PEO thin film (O/K = 64).

[15] J. Bang, S. H. Kim, E. Drockenmuller, M. J. Misner, T. P. Russell, C. J. Hawker, *J. Am. Chem. Soc.* **2006**, *128*, 7622.

[16] T. W. Greene, P. G. M. Wuts, in *Protective Groups in Organic Synthesis*, Wiley, New York **1999**.

[17] S. Yurt, U. K. Anyanwu, J. R. Scheintaub, E. B. Coughlin, D. Venkataraman, *Macromolecules* **2006**, *39*, 1670.

[18] S. H. Kim, M. J. Misner, T. P. Russell, *Adv. Mater.* **2004**, *16*, 2119.

[19] S. H. Kim, M. J. Misner, L. Yang, O. Gang, B. Ocko, T. P. Russell, *Macromolecules* **2006**, *39*, 8473.

[20] A. V. Ruzette, P. Soo, D. R. Sadoway, A. M. Mayes, *J. Electrochem. Soc.* **2001**, *148*, A537.

[21] H. Epps, III, T. S. Bailey, H. D. Pham, F. S. Bates, *Chem. Mater.* **2002**, *14*, 1706.

[22] M. A. Ratner, D. F. Shriver, *Chem. Rev.* **1988**, *88*, 109.

[23] M. Bessodes, D. Komiotis, K. Antonakis, *Tetrahedron Lett.* **1986**, *27*, 579.

[24] R. T. Blickenstaff, *J. Am. Chem. Soc.* **1960**, *82*, 3673.

[25] M. MacCoss, D. J. Cameron, *Carbohydr. Res.* **1978**, *60*, 206.

[26] N. C. Yung, J. J. Fox, *J. Am. Chem. Soc.* **1961**, *83*, 3060.

[27] R. A. Segalman, H. Yokoyama, E. J. Kramer, *Adv. Mater.* **2001**, *13*, 1152.

[28] R. A. Segalman, A. Hexemer, E. J. Kramer, *Phys. Rev. Lett.* **2003**, *91*, 196 101.

[29] J. Y. Cheng, C. A. Ross, E. L. Thomas, H. I. Smith, G. J. Vancso, *Adv. Mater.* **2003**, *15*, 1599.

[30] J. Y. Cheng, A. M. Mayes, C. A. Ross, *Nat. Mater.* **2004**, *3*, 823.

[31] D. Sundrani, S. B. Darling, S. J. Sibener, *Nano Lett.* **2004**, *4*, 273.

[32] D. Sundrani, S. B. Darling, S. J. Sibener, *Langmuir* **2004**, *20*, 5091.

[33] M. R. Hammond, E. Cochran, G. H. Fredrickson, E. J. Kramer, *Macromolecules* **2005**, *38*, 6575.